SIZE DEPENDENCE OF GEOMETRIC STRUCTURES AND ELECTRONIC PROPERTIES OF 3-BROMOPYRIDINE N-OXIDE INVESTIGATED BY DENSITY FUNCTIONAL THEORY MOLECULAR DYNAMIC SIMULATIONS

Pek-Lan Toh [a,*], Jia-Jing Lim [a], Montha Meepripruk [b]

[a]*Department of Electronic Engineering, Faculty of Engineering and Green Technology, Universiti Tunku Abdul Rahman, 31900 Kampar, Perak, Malaysia*
[b]*School of General Science, Institute of Education, Kampheang Phet Rajabhat University, Kampheang Phet 62000, Thailand*

Received 14 March 2017; Revised 19 June 2017; Accepted 26 June 2017

ABSTRACT

In this work, Density Functional Theory (DFT) method was carried out to study the size-dependent structures, stabilities, and electronic properties of 3-Bromopyridine N-Oxide, C_5H_4BrNO molecular system. $(C_5H_4BrNO)_M$ was chosen as a host local environment with the number of molecule size M = 1, 2, 4, and 8. The stability of $(C_5H_4BrNO)_M$ was obtained using geometry optimization calculation. Four equilibrium structures obtained were then used to calculate total energy, HOMO-LUMO energy gap, and others. The computed findings show that the calculated geometrical parameters (i.e. bond distances, bond angles, and dihedral angles) for four different molecule size of $(C_5H_4BrNO)_M$ are close to the x-ray crystallography data. From the calculation, the total energy and HOMO-LUMO gap values were observed to decrease when the number of molecule size increases. Using MPA scheme, the computed findings clearly note that the most positive charge is determined to be above +0.292 for the atom of C_3, whereas C_4 atom gets the most negative charge, with the corresponding value of –0.296.

KEYWORDS: *Density Functional Theory; 3-Bromopyridine N-Oxide; Size-dependent structures; Electronic properties*

* Corresponding authors; e-mail: peklan_toh@yahoo.com.my ,Tel: +(605)468-8888, Fax: +(605)466-1313

INTRODUCTION

In recent years, pyridine derivatives have great potential for usage in optoelectronics, namely photodiodes, solar cells, light emitting diodes (LEDs), laser diodes, and others [1–5]. For example, in 2015, the computational and theoretical studies of new pyridine derivatives, i.e. pyridine-furan, pyridine-pyrrole, and pyridine-thiophene oligomers were reported by Sahu and his co-workers [1]. The electronic structures and optoelectronic properties of these pyridine derivatives were determined using Density Functional Theory (DFT) method. In the case of helices, the computed results show that the major contribution to the electron transition is not only from Frontier molecular orbital, it can also from the excitation involving the molecular orbital in the molecular system. Singh *et al*., in 2016 synthesized the new 4-pyridine based monomer and polymer dyes, such as N, N-dimethyl-N4-((pyridine-4yl)methylene) propaneamine (4, monomer) and polyamine-4-pyridyl Schiff base (5, polymer) dyes [3]. The characteristics of these two 4-pyridine based monomer and polymer dyes were then analyzed using SEM, X-ray crystallographic, mass, NMR, IR, and so on. From the observation, the results obtained note that the maximum energy conversion efficiency of polymer dye based ZnO solar cell is higher than that of monomer dye. At the same year, a series of bis-terpyridine isomers (n-TerPyB) was also studied and presented by Watanabe *et al*. [4]. The organic light-emitting devices (OLEDs) were then successfully fabricated using n-TerPyB as an electron-transporter in the study. However, there is a lot of great theoretical frameworks on the pyridine derivatives nowadays [1, 6–9]. In 2010, Shi *et al*. studied the electronic structures and optoelectronic properties of a series of blue-emitting Iridium (III) complexes, namely $(dfppy)_2Ir(pyN_2)$, $(dfppy)Ir(pyN_2)_2$, and $(fpmb)_2Ir(pyN_3)$ [dfppyH: 2-(2,4-difluorophenyl)pyridine; pyN_2H: 5-

(2-pyridyl)-3-trifluoromethylpyrazole; Hfpmb: 1-(4-fluorophenyl)-2,3-dihydro-3-methyl-1H-benzo [d]imidazole; and pyN_3H: 2-(5-(trifluoromethyl)-2H-1,2,4-triazol-3-yl)pyridine] using computational DFT molecular dynamic simulations [6]. The calculated data clearly shows that the molecular compounds with pyridine ligands have great influence on the photophysical properties, i.e. energy gap, emission spectra, absorption spectra, and others. In addition, $(dfppy)_2Ir(pyN_2)$ is the best candidate for usage in blue-emitting material. Zhao *et al*., in 2014, investigated the external electric field effects on the surface-enhanced Raman scattering of pyridine–metal materials with employing the technique of DFT [9]. In this study, the geometrical structures and polarizabilities of pyridine–metal complexes is found to be slightly change when the external field is applying with the orientation parallel or antiparallel of dipole moment. As far as we know there is no general reports on the electronic properties of 3-Bromopyridine N-Oxide, C_5H_4BrNO have yet been published. To improve our pyridine ligand knowledge, Density Functional Theory (DFT) calculation was carried out to study the size dependence of geometric structures, energetics, and others electronic properties of C_5H_4BrNO molecular system.

MATERIALS AND METHODS

In this study, all computational Density Functional Theory (DFT) calculations were carried out using Gaussian 09 software. A single molecule of 3-Bromo-Pyridine N-Oxide, C_5H_4BrNO was chosen as a local environment. Fig. 1 presents the diagram of C_5H_4BrNO molecular system. Using the DFT hybrid functional (B3LYP) with employing the basis set of 6–311++G**, the geometry optimization calculation was carried out to find the local energy minimum of C5H4BrNO molecular system. The optimized geometry structure was then used to determine the total energy, the frontier molecular orbital energies (i.e. Highest Occupied Molecular Orbital (HOMO) and Lowest Unoccupied Molecular Orbital (LUMO) energies), atomic charge, and others. In order to study the intermolecular interaction effect, the molecule size of $[C_5H_4BrNO]_M$ molecular system were further explored up to M = 2, 4, and 8. Fig. 2(a) - 2(c) show the diagrams of $[C_5H_4BrNO]_M$ with the molecule size number, M = 2, 4, and 8. The geometry optimization calculation was carried out to find the local energy minimum of $[C_5H_4BrNO]_M$ molecular system at DFT/B3LYP/6-311++G** level of theory. The optimized geometries were then employed to calculate the total energy, HOMO and LUMO energies, and so on.

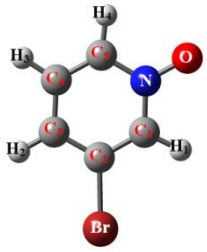

Fig. 1 Single molecule of 3-Bromo-Pyridine N-Oxide.

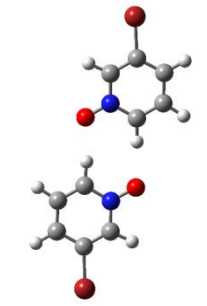

2(a)

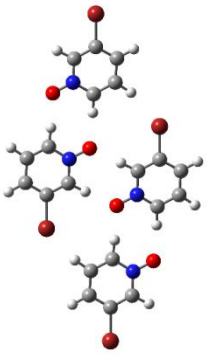

2(b)

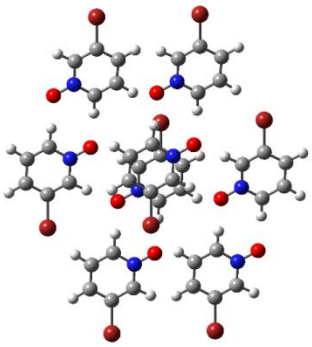

2(c)

Fig. 2 Structures of $[C_5H_4BrNO]_M$ with the molecule size number: (a) M = 2, (b) M = 4, and (c) M = 8.

RESULTS AND DISCUSSION

Table 1 presents the calculated geometrical parameters (i.e. bond length, bond angle, and dihedral angle) of $[C_5H_4BrNO]_M$ (M = 1, 2, 4, and 8). From the table, it can be found that all computed geometrical parameters obtained are in good agreement with the bulk data [2]. For four different molecule sizes of $[C_5H_4BrNO]_M$, the calculated C-C bond are 0.8% - 1.1% longer than those of experimental values. In the case of C_5-N bond, our calculation results show that a single molecule of C_5H_4BrNO has the largest bond length. The corresponding C_5-N bond distance is 1.5% greater than that of measurement data (1.369Å). While for the other four molecule sizes, the C_5-N bond is only 1.2% longer than that of bulk value. A similar trend is found on N-O bond. The N-O bond distance for the single molecule of C_5H_4BrNO is 2.2% shorter than that of experimental data (1.302Å), whereas the other four molecule sizes is only 1.3% smaller that measurement value. Again, it can be noted that for all molecule sizes of $[C_5H_4BrNO]_M$, the computed C_2-Br bonds obtained are 1.2% larger than that of experimental result (1.885Å). With increasing molecule size of $[C_5H_4BrNO]_M$, the results show that the computed bond angle obtained is also close to the bulk result. For example, the bond angles of C_1-C_2-O in the cases of single and two molecules are determined to be about 118.12° and 118.21°, respectively. These two C_1-C_2-O bond angles obtained are 0.7% smaller than that of measurement result. While for the other two molecule sizes (M = 4 and 8), the corresponding C_1-C_2-O bond angles are only 0.6% smaller than that of measurement result. Furthermore, the C_1-N-O bond angle is also predicted to be about 120.35° in the single molecule of C_5H_4BrNO. This C_1-N-O bond angle obtained is typically a much greater angle as compared to the other three molecule sizes (M = 2, 4, and 8). The calculated C_1-N-O bond C_1-N-O bond angle (118.99°). A similar trend is observed for the dihedral angle of C_2-C_1-N-O as shown in the table. Four computed C_2-C_1-N-O dihedral angles obtained are only slightly greater than that of bulk value (178.28°).

Table 1 Geometrical parameters of $[C_5H_4BrNO]_M$ with the number of molecule size, M = 1, 2, 4 and 8

	DFT/B3LYP/6-311G**				Experiment [2]
	M = 1	M = 2	M = 4	M = 8	
Bond distance (Å)					
C_1-C_2	1.382	1.382	1.382	1.382	1.367
C_2-C_3	1.391	1.391	1.391	1.390	1.390
C_3-C_4	1.394	1.393	1.393	1.393	1.381
C_4-C_5	1.380	1.381	1.381	1.381	1.369
C_5-N	1.372	1.369	1.369	1.369	1.352
C_2-Br	1.909	1.908	1.908	1.908	1.885
N-O	1.273	1.286	1.285	1.286	1.302
Bond angle (°)					
C_1-C_2-O	118.12	118.21	118.27	118.27	119.00
C_1-N-O	120.35	119.56	119.61	119.62	118.99
Dihedral angle (°)					
C_2-C_1-N-O	178.31	178.29	178.29	178.29	178.28

Table 2 summarizes that the total and Frontier molecular orbital energies of $[C_5H_4BrNO]_M$ with the number of molecule size, M = 1, 2, 4, and 8. As a result, we obtained that the total energy decreases with increasing the molecule size number of $[C_5H_4BrNO]_M$. For a single molecule of C_5H_4BrNO, the calculated total energy is predicted to be –78833.529 eV, while the energy values of –157667.344 eV, –315334.887 eV, and –630669.801 eV are obtained for the other three molecule sizes (M = 2, 4, and 8), respectively. In this paper,

Frontier molecular orbital's (FMOs) energies are very important. This is because it helps to obtain the information about stability, chemical reactivity, optical, and electrical properties of the system. For the electronic structure calculations, we also observed that HOMO-LUMO energy gap decreases with increasing the number of molecule size. As can be seen from the table, the HOMO-LUMO gap values are determined to be 4.606 eV, 4.564 eV, 4.541 eV, and 4.517 eV, respectively for the molecule size, M = 1, 2, 4, and 8. Also, Frontier molecular orbital diagram of C_5H_4BrNO is presented in Fig. 3. Using DFT/B3LYP/6-311++G** level of theory, the computed results in Fig. 3(a) show that HOMO has mostly p character, respectively, comes from the orbitals of O, C_1, C_3, and C_5 atoms. While LUMO has mostly p character, and the electron distributions are focused on the phenyl ring. In Fig. 3(c) and Fig. 3(d), the similar results are also obtained when the molecular size increases. Since there are no experimental data on the bad gap of the title compound, these results can use as a reference to measure the data of future experiments.

Table 2 Total and Frontier molecular orbital energies (eV) of $[C_5H_4BrNO]_M$ (M = 1, 2, 4, and 8)

	M = 1	M = 2	M = 4	M = 8
Total energy	–78833.529	–157667.344	–315334.887	–630669.801
HOMO	–6.553	–6.485	–6.470	–6.443
LUMO	–1.947	–1.920	–1.928	–1.926
HOMO-LUMO gap	4.606	4.564	4.541	4.517

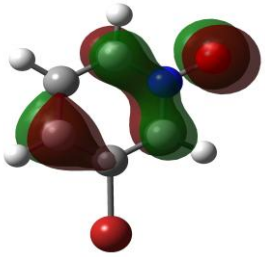

3(a) HOMO (–6.553 eV)

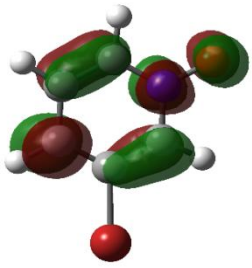

3(b) LUMO (–1.947 eV)

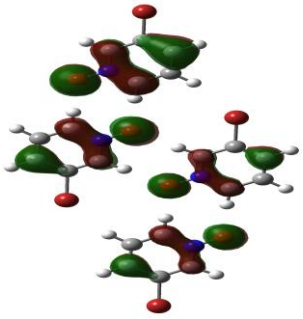

3(c) HOMO (-6.470 eV)

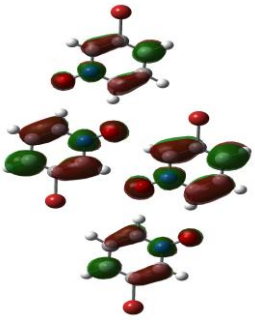

3(d) LUMO (-1.928 eV)

Fig. 3 Frontier molecular orbitals of 3-Bromo-Pyridine N-Oxide: (a) HOMO with molecular size of M = 1, (b) LUMO with molecular size of M = 1, (c) HOMO with molecular size of M = 4, and (d) LUMO with molecular size of M = 4.

To know the molecular reactive of C5H4BrNO molecular system, the molecular electrostatic potential (MEP) surface is presented in Fig. 4. From the figure, it can be noted that the different colored surfaces is represented by the different MEP energy levels. In this work, the lowest electrostatic potential energy regions are only focused around O and Br atoms, whereas all hydrogen and C_3 atoms get the highest electrostatic potential energy in this study. Using a scheme of Mulliken Population Analysis (MPA), the atomic charge distribution of

C_5H_4BrNO molecular system is illustrated in Fig. 5. The atom of C_3 is the most positive charge, with the corresponding value of +0.292. While the most negative charge (–0.296) is obtained on C_4 atom as shown in the figure.

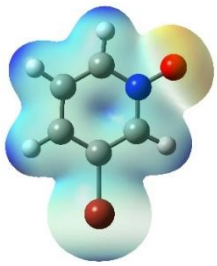

Fig. 4 Molecular electrostatic potential (MEP) surface of 3-Bromo-Pyridine N-Oxide.

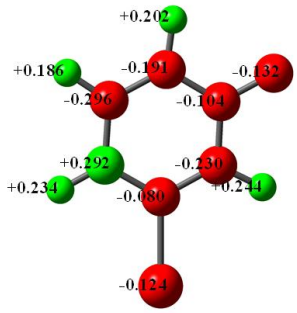

Fig. 5 Atomic charge distribution of 3-Bromo-Pyridine N-Oxide molecular system.

CONCLUSION

The molecule size dependence on the geometric structures and electronic properties of 3-Bromo-Pyridine N-Oxide molecular system was studied using DFT molecular dynamic simulations. Using DFT/B3LYP/6-311++G** calculation, the overall computed geometrical parameters for four different molecule sizes of $[C_5H_4BrNO]_M$ (M = 2, 4, and 8) are close to the bulk data [2]. With increasing the number of molecule size, it can be seen that the calculated total and HOMO-LUMO energies are found to be decrease. Thus, the results from MPA scheme summarizes that C_3 atom is the most positive charge (+0.292), whereas the most negative (–0.296) is found on the atom of C_4. Furthermore, we are currently carried out the point charge method on a larger molecule size of $[C_5H_4BrNO]_M$ system.

ACKNOWLEDGEMENTS

This research is supported by Universiti Tunku Abdul Rahman Research Fund IPSR/RMC/ UTARRF/2015-C2/T05.

REFERENCES

[1] H. Sahu, S. Gupta, P. Gaur, A.N. Panda, Structure and optoelectronic properties of helical pyridine-furan, pyridine-pyrrole and pyridine-thiophene oligomers, Phys. Chem. Chem. Phys. 17 (2015) 20647–20657.

[2] M.G. Hutchinson, W.E. Lynch, C.W. Padgett, Crystal structure of 3-bromopyridine N-oxide, Acta Cryst. E. 71 (2015) o869.

[3] S. Singh, T. Raj, A. Singh, N. Kaur, Optoelectronic and photovoltaic performances of pyridine based monomer and polymer capped ZnO dye-sensitized solar cells, J. Nanosci. Nanotechnol. 16(6) (2016) 5975–5983.

[4] Y. Watanabe, R. Yoshioka, H. Sasabe, T. Kamata, H. Katagiri, D. Yokoyamaab, J. Kido, Fundamental functions of peripheral and core pyridine rings in a series of bis-terpyridine derivatives for high-performance organic light-emitting devices, J. Mater. Chem. C. 4 (2016) 8980–8988.

[5] X.J. Yin, G.H. Xie, T. Zhou, Y.P. Xiang, K.L. Wu, J.G. Qina, C.L. Yang, Simple pyridine hydrochlorides as bifunctional electron injection and transport materials for high-performance all-solution-processed organic light emitting diodes, J. Mater. Chem. C. 4 (2016) 6224–6229.

[6] L.L. Shi, B. Hong, W. Guan, Z.J. Wu, Z.M. Su, DFT/TD-DFT study on the electronic structures and optoelectronic properties of several blue-emitting iridium(III) complexes, J. Phys Chem. A. 114(24) (2010) 6559–6564.

[7] S.S. Zhao, L.L. Shi, Z.M. Su, Y. Geng, L. Zhao, TD-DFT studies on electronic and spectral properties of platinum(II) complexes with phenol and pyridine groups, Chin. Univ. 29(2) (2013) 361–365.

[8] Z.G. Niu, L.R. He, L. Li, W F. Cheng, X Y. Li, H.H. Chen, G.N. Li, Synthesis, characterization and DFT studies of two new π-conjugated pyridine-based tetrathiafulvalene derivatives, Acta Chim. Slov. 61 (2014) 786–791.

[9] X.M. Zhao, M.D. Chen, DFT study on the influence of electric field on surface-enhanced raman scattering from pyridine-metal complex, J. Raman Spectrosc. 45(1) (2014) 62–67.

[10] M.J. Frisch, G.W. Trucks, H.B. Schlegel, G.E. Scuseria, M.A. Robb, J.R. Cheeseman, et al. Gaussian 09, Revision E.01, Gaussian Inc, United States of America, 2004.